Mem. Fac. Eng., Osaka City Univ., Vol. 39, pp. 77－87 (1998)

# Spatial Distribution of He I 5876Å & He II 4686Å Line Radiation of TPD-S Plasma and Its Computer Simulation

**Hiroshi Tsuji* , Masatoshi Mita* , Mikio Mimura* ,**
**Takashi Kobuchi** and Kuninori Sato****

(Received September 30, 1998)

## Synopsis

The plasma created by the TPD-S machine of National Institute for Fusion Science changes its shape depending on the discharge current and the density in the experimental region. We measured the spatial distribution of the intensity of He atomic line (5876Å) and ionic line (4686Å) emitted by the plasma. In order to explain the distribution, we carried out a numerical simulation by integrating the rate equations. A suitable electron temperature distribution may explain the measured spatial distribution of the line intensity.

Keywords : stationary plasma , TPD-S machine , rate equation , digital camera

## Introduction

The TPD-S (Test Plasma by Direct current discharge for Spectroscopy) machine of National Institute for Fusion Science was built for the fundamental study of plasma spectroscopy. It creates a plasma with high degree of ionization and small noise.

The shape of the plasma created by this machine considerably changes when the discharge current and the introduced gas density are varied. For example, it is a simple cylindrical plasma whose emission strongly extends along the center axis or double structure of a cylindrical plasma and halo around it. In some condition, the emission spatially disappears and then appears once again. We took monochromatic image of helium line spectrum of these plasmas by a digital camera and interference filters. The spatial distribution of the intensity of these line spectrums is obtained from the image data. To explain the spatial distributions, we made a computer simulation on the helium line intensity using rate equations. When we assumed a suitable electron temperature distribution for each plasma discharge current, the calculated spatial distribution of the light intensity resembles to that of the experiment data.

* Department of Applied Physics, Faculty of Engineering

** National Institute for Fusion Science (NIFS)

## Experimental Setup and Result

The experimental setup is shown schematically in Fig 1. The discharge is made between a cathode and an anode which has a hole in the center. The floating electrodes are placed between the cathode and the anode to stabilize the pressure gradient and to smooth the electric potential. The magnetic field is applies to confine the plasma on center axis and to introduce the plasma to the anode hole. Helium gas is introduced from the back of the cathode. The discharge voltage is 150V~160V and the discharge current is 10A~40A. The plasma flows through the anode hole to the experimental region by the pressure gradient.

Three examples of plasma shape are shown in Fig. 2. They are taken from the window by the digital

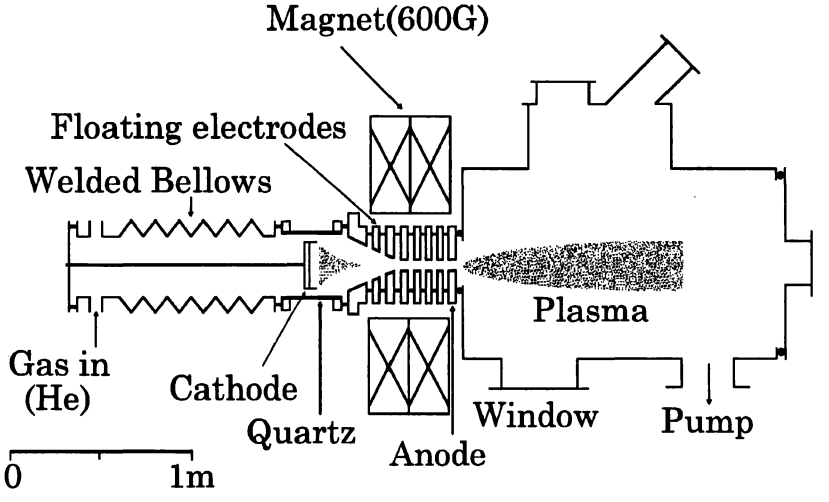


Fig. 2 The schematic drawing of TPD-S machine.

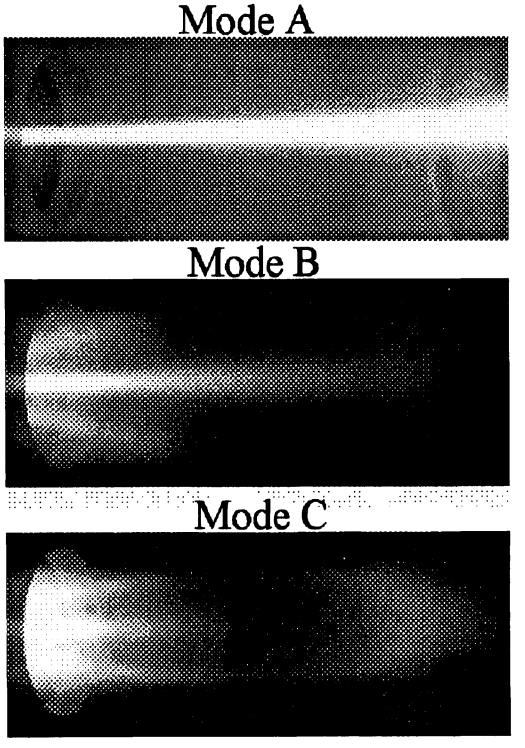


Fig. 1 The shape of mode A,B,C plasma.

camera (FUJIX DS-505) as a usual picture without the interference filter. Mode A plasma in Fig.2 is created by 150V-35A discharge. The gas pressure in the discharge region and the experiment region is 5 Torr and $5 \times 10^{-4}$ Torr respectively. A cylindrical plasma with a diameter of about 8mmϕ which equals to that of anode hole flows out through the anode hole. Its emission extends along the center axis. Mode B plasma is created by 155V-25A discharge. The gas pressure in the discharge region and the experiment region is 10 Torr and $1 \times 10^{-3}$ Torr respectively. There is a core plasma whose diameter is equal to that of anode hole. Enveloping the core plasma, there is also a halo plasma whose diameter is approximately 80mmϕ. It is seen that both plasma emissions disappear spatially on the way. Mode C plasma is created by 160V-10A discharge. The gas pressure in the discharge region and the experiment region is 20 Torr and $5 \times 10^{-3}$ Torr respectively. Similar to the mode B plasma, a core plasma and a halo plasma are seen. Both the core and the halo plasma spatially disappear, but appear once again.

Next, we took monochromatic images of the plasma using the digital camera with interference filters (TOSHIBA KL59 and KL46). From these images we got the spatial distributions of the intensity of the atomic line (5876Å) and the ionic line (4686Å). Although the resolving power of the interference filter is low ($\lambda_{1/2}$=140Å), the filter is applicable because other line spectrum doesn't appear near 5876Å and 4686Å line. The image consists of 1280×1000 pixels. It is stored in an uncompressed TIFF format file (24bit color mode). To analyze the image, we have used NEOSLASH program[1] developed at our group. The program is written in Quick Basic of NEC PC 9801 computer. Using this program, it is possible to display x- or y-cross section, bird's-eye view, histogram and so on.

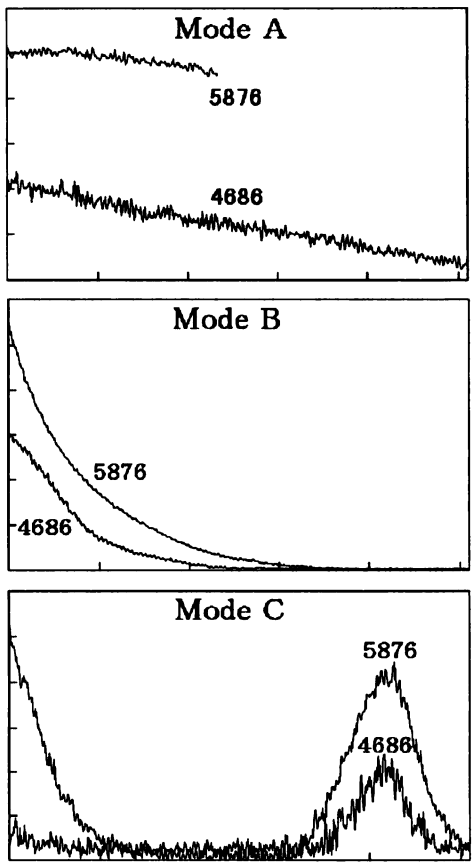


Fig.3 The intensity distribution of 5876Å line and 4686Å line along the center axis for A,B,C plasma.

At first we analyze the intensity distribution along the center axis. We omit the data near the anode hole because of the saturation of CCD and the reflection of light by the wall. We performed Abel inversion of the two dimensional monochromatic plasma image of HeI 5876Å and HeII 4686Å. Thus obtained intensity distributions along the center axis are shown in Fig.3. In mode A plasma the intensity of both 5876Å and 4686Å lines extends along the center axis and decrease monotonously. We could not get the right half of the 5876Åline intensity because of an experimental mistake. In mode B plasma, the intensity of both lines decreases rapidly and disappears. In mode C plasma, 5876Å line disappears once and then appears again. As for the 4686Å line, only one peak is seen in this range. But there is bigger peak near the anode, where we omit because of saturation. Therefore the 4686Å line also disappears once and then appears again in the similar way to 5876Å line.

## Computer Simulation using the Time History Method

To explain the intensity distributions of these line-spectra, we calculate them using the time history method by rate equations. Time history method is originally applied to transient plasmas like Pinch or Tokamak[2][3]. To apply this method to a stationary plasma, we used the relation between time and position of plasma in a following way. As shown in Fig.4, the plasma flows out of the anode hole and moves as a function of time. The

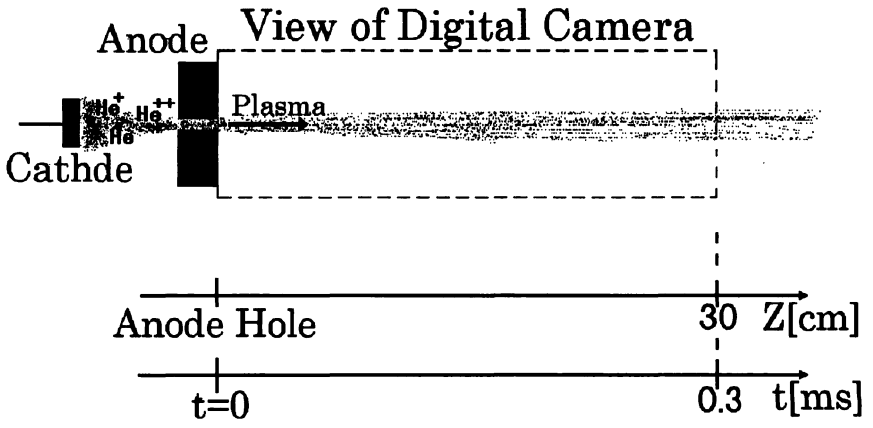


Fig. 4 The image view of the conversion the location of the plasma to the time.

plasma traverses the field of view of the digital camera (30 cm) in about 0.3 ms due to the thermal velocity. We solve the rate equations in the time interval between $t$ =0 ms and 0.3 ms, where $t$ =0 ms corresponds to the position of anode hole. The rate equations to be solved are;

$$\frac{dn_1}{dt} = -s_1 n_e n_1 + r_1 n_e n_2 - \frac{n_1}{\tau}$$

$$\frac{dn_2}{dt} = s_1 n_e n_1 - r_1 n_e n_2 - s_2 n_e n_2 + r_2 n_e n_2 - \frac{n_2}{\tau}$$

$$\frac{dn_3}{dt} = s_2 n_e n_2 - r_2 n_e n_3 - \frac{n_3}{\tau}$$

where $n_1, n_2$ and $n_3$ mean the density of $He, He^+$ and $He^{2+}$ respectively, $s_1$ and $s_2$ are the ionization rate coefficient from $He$ to $He^+$ and from $He^+$ to $He^{2+}$ respectively, $r_1$ and $r_2$ are the recombination rate coefficient from $He^+$ to $He$ and $He^{2+}$ to $He^+$ respectively. To include the density decrease due to plasma expansion, we introduce an attenuation coefficient τ.

Grotorian diagram of $He$ and $He^+$ is shown in Fig.5. Only the excitation from the ground state and

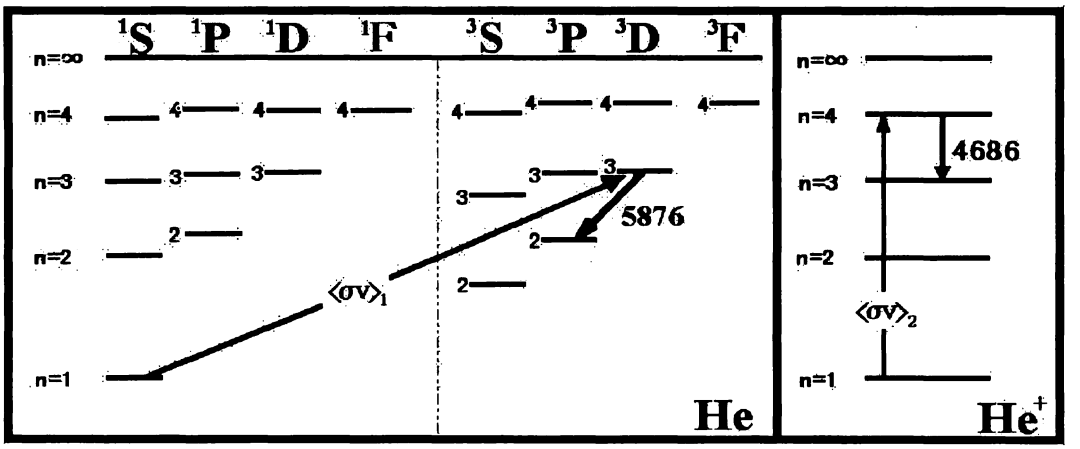


Fig. 5 The Grotorian diagram of $He$ and $He^+$ in the range from the quntum number of n=1 to n=4. The 5876Å line is emitted by the transition from $3^3D$ to $2^3P$ and the 4686Å line is from $n$=4 to $n$=3.

recombination from the continuous level are taken into account. The intensity of 5876Å line and 4686Å line is written as;

$$I(5876\text{Å}) = n_e \langle \sigma v \rangle_1 n_1 + n_e G R_1(3) n_2$$

$$I(4686\text{Å}) = \left( n_e \langle \sigma v \rangle_2 n_2 + n_e R_2(4) n_3 \right) \times \frac{A_{43}}{A_{41} + A_{42} + A_{43}}$$

where $\langle \sigma v \rangle_1$ and $\langle \sigma v \rangle_2$ mean the excitation rate coefficient of $He$ and $He^+$ respectively, $R_1(3)$ is the recombination rate coefficient from the continuous level of $He^+$ to the $n$=3 state of $He$, $R_2(4)$ is that from the continuous state of $He^{2+}$ to the $n$=4 state of $He^+$, $G$ is the ratio of the statistic weight of $3^3D$ state to the sum of that of all the $n$=3 levels ( i.e. $G = 7/(1+3+5+3+5+7) = 0.292$ ) and $A_{ij}$ is the transition probability between $i$ state and $j$ state.

Therefore, the emission intensity depends on the eleven parameters; the electron density $n_e$, the atom and ion density $n_1, n_2, n_3$, the excitation rate coefficients $\langle \sigma v \rangle_1, \langle \sigma v \rangle_2$, the recombination rate coefficients $r_1, r_2$, the ionization rate coefficients $s_1, s_2$ and the attenuation coefficient τ. But as shown below, it actually depends on the three independent parameters; electron temperature $Te$, the sum of the atom and ion density $N (= n_1 + n_2 + n_3)$ and the attenuation coefficient τ.

i) The Electron Density

Because the plasma is electrically neutral, the electron density is derived from the ion density; $n_e = n_2 + 2 \cdot n_3$.

ii) The Ionization, Excitation and Recombination rate Coefficients

The ionization rate coefficient is given as the following relation[4];

$$S_i = e^{-I_i/Te}\left(\frac{Te}{I_i}\right)^{1/2}\sum_{n=0}^{5} a_n\left(\log_{10}\left(\frac{Te}{I_i}\right)\right)^n \quad cm^3/s,$$

where $Te$ is the electron temperature, $I_i$ is the ionization potential and $a_n$ is a coefficient which depends on the atom species. Figure 6 shows the dependence on the electron temperature.

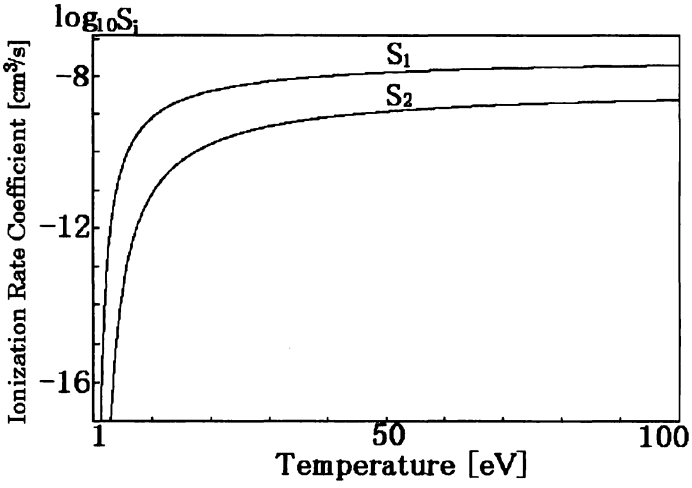


Fig. 6 The ionization rate coefficient.

The excitation rate coefficient is given as the following relation[5];

$$\langle\sigma v\rangle_Z = 1.70\times10^{-3}(Te\cdot 11600)^{-1/2}E_{ij}^{-1}f_{ji}\cdot P(y)\cdot\exp(-y) \quad cm^3/s,$$

$$P(y) = A + (By - Cy^2 + D)\cdot\left(\ln\left(\frac{y+1}{y}\right) - \frac{0.4}{(y+1)^2}\right) + Cy,$$

where $E_{ij}$ is the excitation energy, $f_{ij}$ is the oscillator strength, $A, B, C$ and $D$ are the coefficients of Mewe, and $y = I_i / Te$. $Z$ is unity or two. Figure 7 shows the dependence on the electron temperature.

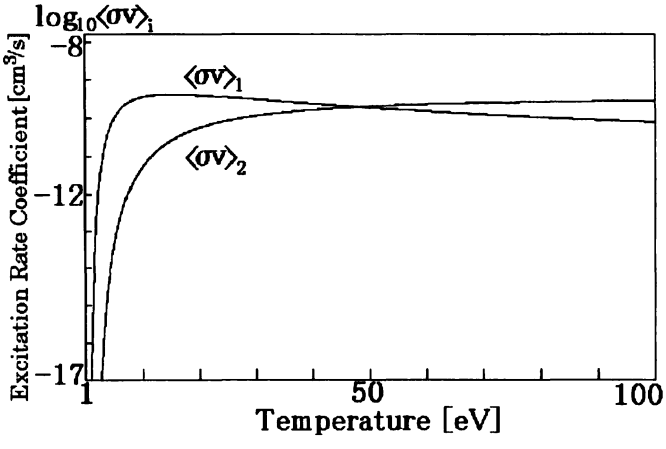


Fig. 7 The excitation rate coefficient

The recombination rate coefficient from $He^+$ to $He$ and from $He^{2+}$ to $He^+$ are given;

$$r_1 = 2 \cdot R_1(1) + \sum_{i=2}^{\infty} R_i(i) \text{ and } r_2 = \sum_{i=1}^{\infty} R_2(i)^{(6)},$$

where

$$R_Z(i) = 2.607 \times 10^{-12} \frac{Z^4}{i^3} \cdot (Te)^{-3/2} \cdot \left( \log \frac{y+1}{y} - \frac{0.4}{(y+1)^2} \right) \quad cm^3/s^{(7)}.$$

Figure 8 shows the dependence on the electron temperature.

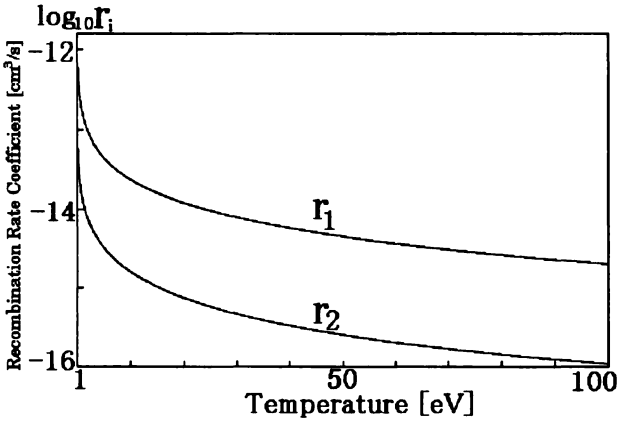


Fig. 8 The recombination rate coefficient

iii) The Attenuation Coefficient

The plasma density near the center axis decreases because the plasma flows with expansion. To include this effect in the equations, we introduced the attenuation coefficient.

iv) The Initial Values of the Density of Atom and Ions

The initial values of $n_1, n_2$ and $n_3$ can't measured. We assume that the plasma in the discharge region is stationary; $dn_i/dt = 0$. Then from the rate equations and $N = n_1 + n_2 + n_3$, we get following relations;

$$\begin{aligned} n_1 &= r_1 \cdot r_2 / s_1 \cdot N / (r_1 \cdot r_2 / s_1 + s_2 + r_2) \\ n_2 &= r_2 \cdot N / (r_1 \cdot r_2 / s_1 + s_2 + r_2) \\ n_3 &= s_2 \cdot N / (r_1 \cdot r_2 / s_1 + s_2 + r_2) \end{aligned} ,$$

therefore if the initial values of $N$ and electron temperature are given, the initial values of $n_1, n_2$ and $n_3$ are obtained.

Now the intensity distribution of the emission can be calculated if the electron temperature distribution, the attenuation coefficient, and the sum of the atom and the ion density are given. The data necessary for the calculation are summarized in Table 1. We calculated the line intensity distribution by changing these three parameters. A good agreement with the experimental result was obtained when $\tau$=0.04 ms. We fixed this parameter and changed the initial value of $N$ and the electron temperature distribution so that the calculated intensity distribution agrees to the measured intensity distribution.

(a) Data necessary for the calculation of the ionization rate coefficients

| | I.P.[eV] | $a_0$ | $a_1$ | $a_2$ | $a_3$ | $a_4$ | $a_5$ |
|---|---|---|---|---|---|---|---|
| $He$ | 24.587 | 1.500E-8 | 5.666E-10 | -6.082E-9 | -3.589E-9 | 1.553E-9 | 1.320E-9 |
| $He^+$ | 54.416 | 3.436E-9 | -1.687E-9 | -6.924E-10 | 9.786E-11 | 1.559E-10 | 6.224E-11 |

(b) Date necessary for the calculation of the recombination rate coefficients

· $He^+ \rightarrow He$

| Level | I.P.[eV] | Statistic Weight | Level | I.P.[eV] | Statistic Weight | Level | I.P.[eV] | Statistic Weigh |
|---|---|---|---|---|---|---|---|---|
| $1^1S$ | 24.59 | 1 | $3^1D$ | 1.51 | 5 | $4^1D$ | 0.85 | 5 |
| $2^1S$ | 1.97 | 1 | $3^3S$ | 1.83 | 3 | $4^1F$ | 0.85 | 7 |
| $2^1P$ | 3.37 | 3 | $3^3P$ | 1.54 | 5 | $4^3S$ | 0.96 | 3 |
| $2^3S$ | 4.73 | 3 | $3^3D$ | 1.48 | 7 | $4^3P$ | 0.84 | 5 |
| $2^3S$ | 3.59 | 5 | $4^1S$ | 0.91 | 1 | $4^3D$ | 0.82 | 7 |
| $3^1S$ | 1.67 | 1 | $4^1P$ | 0.84 | 3 | $4^3F$ | 0.82 | 9 |
| $3^1P$ | 1.50 | 3 | | | | | | |

· $He^{2+} \rightarrow He^+$

| Level | I.P.[eV] | Transition Probability[$10^8 s^{-1}$][8] | Level | I.P.[eV] |
|---|---|---|---|---|
| $n=4$ | 3.402 | $1.438(A_{43})$ | $n=3$ | 6.047 |
| | | $1.347(A_{42})$ | $n=2$ | 13.606 |
| | | $2.045(A_{41})$ | $n=1$ | 54.402 |

(c) Date necessary for the calculation of the excitation rate coefficients

| Excitation Transition | Excitation Energy[eV] | Oscillator Strength | Mewe's Coefficients[4] |
|---|---|---|---|
| $He(1^1S \rightarrow 3^3D)$ | 23.105 | 0.0734 | A=B=D=0,C=0.1 |
| $He^+(n=1 \rightarrow n=4)$ | 51.020 | 0.0290 | A=0.25,B=0.04,C=0,D=0.28 |

Table 1 Data necessary for calculating the ionization, recombination and excitation rate coefficients.

The result of the calculation for the mode A plasma is shown in Fig.9. The top shows the electron temperature, which is varied from 5.5 eV to 5 eV in 0.3 ms. The center shows the density. It is seen that the $He^+$ ion is dominant in this temperature region. Because of the attenuation coefficient, all of the $He$, $He^+$ and $He^{2+}$ density decrease gradually. The excitation rate coefficient also decreases due to the temperature drop. So the intensity of both of the atomic 5876Å line and ionic 4686Å line also decrease.

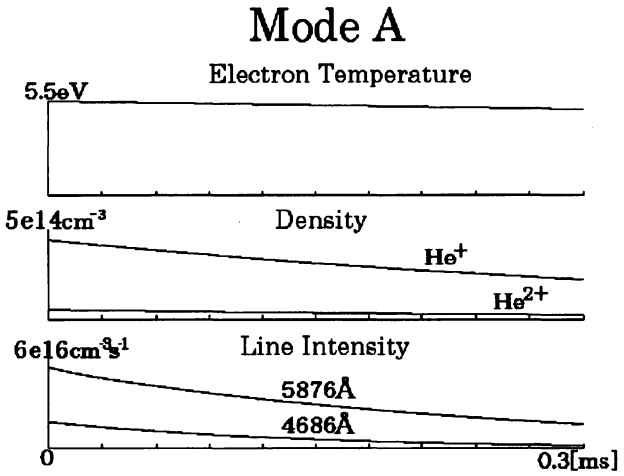


Fig. 9 The simulation result of the mode A plasma

The result of the calculation for mode B plasma is shown in Fig.10. This time, the temperature drops exponentially from 5.5 eV to 1.0 eV in 0.3 ms. Similar to the mode A case, the $He^{+}$ and $He^{2+}$ density decrease. However, recombination takes place as a result of the sharp temperature drop and the $He$ density increases. Because of this density increase, the decrease of 5876Å line intensity is small near the anode hole. Although the recombination takes place, the main process for the emission of the 5876Å line in this temperature region is excitation. Thereafter, the 5876Å line decreases and disappears before 0.3 ms due to low temperature. As for the 4686Å line, because both of the decrease of $He^{+}$ density and the excitation rate coefficient, its emission disappears as soon as the plasma flows out of the anode hole. The calculated result differs from the measured result, in which the 4686Å line disappears in similar way to the 5876Å line as shown in Fig.3.

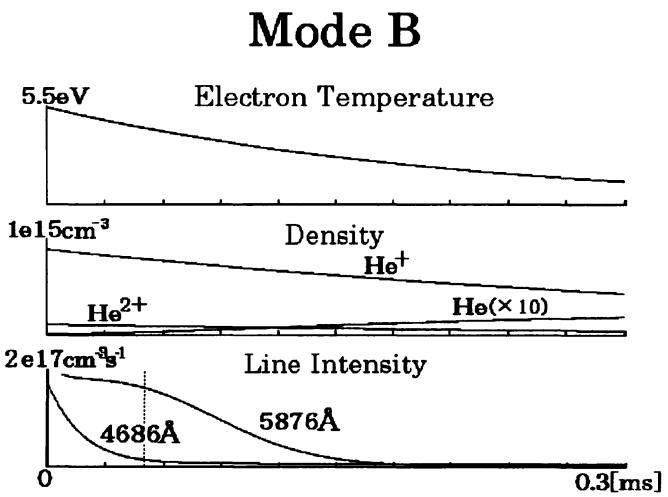


Fig. 10 The simulation result of the mode B plasma

The result of the calculation for mode C is shown in Fig.11. This time, the temperature drops exponentially from 5.5 eV to 1.2 eV in 0.12 ms and thereafter drops from 1.2 eV to 0.1 eV in 0.03 ms. When the temperature drops in such a rapid way, the $He$ density increases sharply and the $He^{2+}$ density decreases also sharply. Then recombination occurs more actively than the Mode B case. The intensity of both of the 5876Å line and

the 4686Å line which decreases when the plasma leaves the anode hole, shows a sudden increase. This is in good agreement with the intensity distribution observed in the experiment. Therefore the reappearance of the 5876Å line and the 4686Å may be explained by the recombination due to the rapid electron temperature drop.

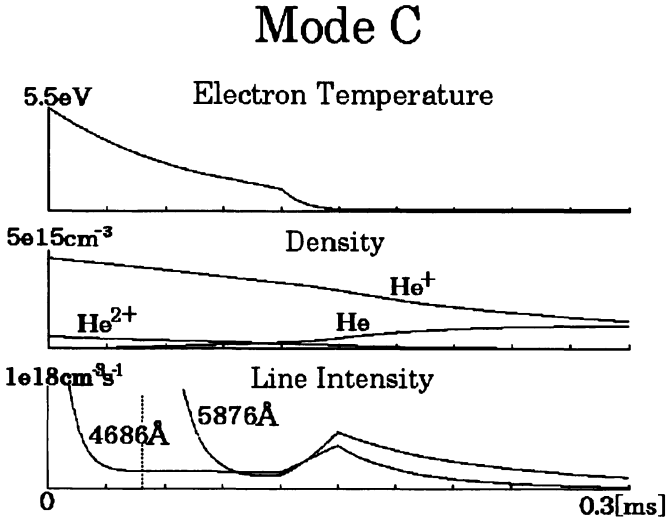


Fig. 11 The simulation result of the mode C plasma

## Conclusion

Using a digital camera and interference filters, we measured the spatial intensity distribution of He I 5876Å line and He II 4686Å line for three discharge modes of TPD-S plasma. By the inverse Abel transformation, the axial intensity distribution of these two lines are obtained.

We performed a simulation of their intensity distribution using rate equations. When we assumed a suitable electron temperature distribution, the initial value of the density of atom and ion, and an attenuation coefficient, the calculated intensity distribution of the two lines agreed quite well to the measured distribution. In this way the reappearance of these two lines observed in the mode C plasma was explained by the recombination process due to a rapid electron temperature drop.

The occurrence of such a rapid temperature drop may be explained by the three-body recombination process. When the plasma is high density and low electron temperature like mode C plasma, the effect of three-body collision and the kinetic energy loss of electrons may not be ignored. Such three-body recombination effect, however, is not taken into consideration so far. The inclusion of this effect in the rate equations will be the next research theme.

## Acknowledgments

This work was carried out under a collaborating research program at the National Institute for Fusion Science.

## References


1) T.Uneyama: Master Thesis (in Japanese), Faculty of Engineering Osaka City University, 1998.
2) M.Mimura, K.Sato, K.Toi and J.Fujita: Jpn.J.Appl.Phys. **25** (1986) 458.
3) M.Mimura, D.D.Meyerhofer, S.F.Paul and P.Young: 7th Symp. on Compact Torus Symposium, Santa-Fe (1985) 25.
4) K.L.Bell, H.B,Gibody, J.G.Hunghes, A.E.Kingston, and F.J.Smith: "Atomic and Molecular Data for Fusion Part I" ,CLM-R216 December (1981).
5) M.Arnaud and R.Rothenflug : Astron.Astrophys.Suppl. **60** (1985) 425.
6) T.Kato: IPPJ-AM-2, June 1977.
7) M.J.Seaton: Mon.Not.R.Astron.Soc. **119** (1959) 81.
8) W.L.Wiese, M.W.Smith, and B.M.Glennon: National Standard Reference Data Series, National Bureau of Standards 4 (1966).